ISSN 2616-5767 Vol.4, Issue 3: 58-63, DOI: 10.25236/AJETS.2021.040307

High Frequency Characteristics of W-band Planar Multi-beam Extended Interaction Circuit

Cui Fu[a], Suye Lü[b,*]

Beijing Institute of Petro Chemical Technology, Beijing 102617, China
[a]email: 2018310570@bipt.edu.cn, [b]email: lvsuye@bipt.edu.cn
**Corresponding author: lvsuye@bipt.edu.cn*

Abstract: *The high frequency characteristics of W-band planar multi-beam extended interaction resonant cavity are studied. The introduction rules of beam tunnels with planar linear arrangement are discussed. It has been found that the introduction position and the number of beam tunnels are limited by the uniformity of the field. Then the transverse and longitudinal mode distributions of the cavity are analyzed. It shows that large transverse dimension and increased number of gaps will significantly affect the frequency interval, and thus affecting the work stability. The field distribution characteristics of different modes are also analyzed. Based on the field shape factor and a set of complex coefficients, a method to describe the distribution characteristics of the field is established.*

Keywords: *Planar multi-beam, multigap resonant cavity, mode distribution, field shape factor.*

1. Introduction

Vacuum electronic amplifier based on extended interaction technology are promising in terahertz band which have the advantages of high peak power, medium bandwidth and small size[1-3]. In recent years, microwave vacuum electronic devices has been developing towards high frequency and high power due to the requirements for high-performance microwave sources. It is a key point that how to greatly improve the power level of the device while the size reduced.

The problem mentioned above can be addressed by using planar distributed electron beam and extended interaction technology. The planar distributed electron beam technology can significantly increase the total current, and the extended interaction technology can form a very short but high gain interaction circuit, thus generating a new device with high power level at high frequency [4-6]. Planar extended interaction devices have the characteristics of planar features which are compatible with micro-machining technology [7,8]. Thus, this kind of devices have great potential for application.

Therefore, extended interaction circuit plays a special role in the design of klystron. The high frequency characteristics of the circuit include field distribution, mode distribution, coupling coefficient, which determine the performance of the circuit. Therefore, the beam-wave interaction is directly affected. The paper discussed the rules of the introduction of beam tunnels, and then mainly analyzed the modes and field shapes of the circuit. The geometric characteristics and operating principle of the barbell multigap resonant cavity were analyzed in Section I. In Section II, the mode distribution of planar multi-beam multigap resonant cavity was analyzed. A method to describe the distribution characteristics of the electric field is established in Section III.

2. Operating principle of the cavity

The structure of the barbell multigap resonant cavity with five beamlets is shown in Figure 1. The axis of the beam tunnels are located on the same plane with a spacing of w_t. The space of the gap is d. The radius of the beam tunnel is R_c.

The barbell resonant cavity is a kind of rectangular one with special structure, which has good uniformity of the electric field in transverse direction. The cause is that the intermediate waveguide works near the cut-off frequency. If the sizes of the coupled cavities are both increased by about a quarter of the wavelength, the resonant frequency of which will be lower than the cut-off frequency. Thus, good uniformity of electric field can be generated in the intermediate waveguide of the barbell cavity.

ISSN 2616-5767 Vol.4, Issue 3: 58-63, DOI: 10.25236/AJETS.2021.040307

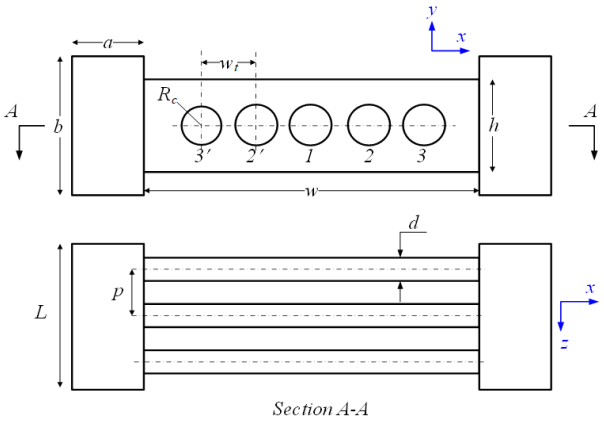

Figure. 1 Schematic of the multigap cavity with five electron beams.

The fundamental 2π mode is selected as the operating mode which is denoted as TM_{110}. The center frequency f_0 is 94.5 GHz, and then the corresponding wavelength is $\lambda = c/f \approx 3.175$mm. The height of the intermediate waveguide h is about $\lambda/2$. The height of the coupled cavities b on both sides is about $h+\lambda/4$. Then, the core design parameters of the barbell resonant cavity are obtained combined with CST simulation, which are as follows: h = 1.585mm, w = 6mm, a = 1.21mm, b = 2.7mm.

Field distribution of 2π mode of the barbell cavity is shown in Figure 2. It can be seen that there is good uniformity of electric field in the transverse direction of the intermediate waveguide region.

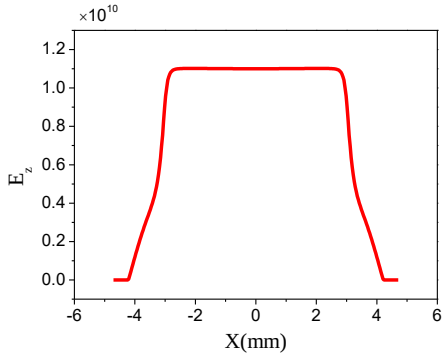

Figure. 2 Transverse field distribution of 2π mode in the barbell resonant cavity.

The good uniformity of the electric field will be destroyed when the beam tunnel is introduced. Figure 3 shows that the field distribution varied with the introduction of a single beam tunnel. It can be seen that the distortion of the electric field is more obvious when the tunnel is not located at the center. Therefore, it is better to introduce the planar multi-beam tunnels symmetrically.

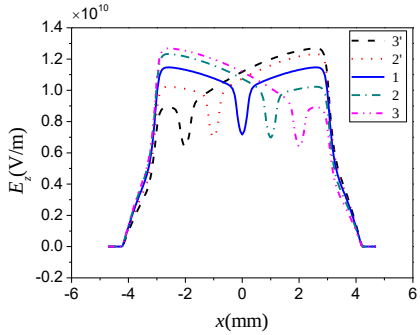

Figure. 3 Transverse field distribution of the cavity varied with a single beam tunnel.

Figure 4 shows the field distribution of three beam tunnels which are introduced symmetrically. The tunnel radius is 0.25 mm. It can be seen that the influence of the field between adjacent tunnels is very small due to the distance between them is relatively bigger. Here, the field intensity in the three beam tunnels is close to each other.

ISSN 2616-5767 Vol.4, Issue 3: 58-63, DOI: 10.25236/AJETS.2021.040307

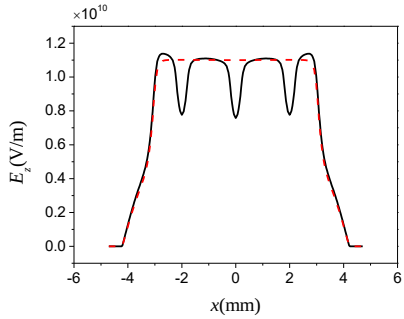

Figure. 4 Transverse field distribution of 2π mode in a planar three-beam barbell resonant cavity.

As shown in Figure 5, the field between beam tunnels will affect each other due to the limit of the transverse size of the circuit when increasing the number of the beam tunnel. Therefore, the radius and the number of the tunnel need to be optimized.

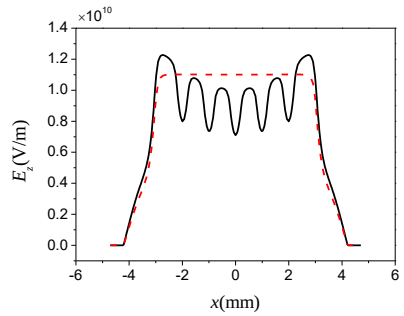

Figure. 5 Transverse field distribution of 2π mode in a planar five-beam barbell resonant cavity.

3. Mode analysis

3.1. Transverse mode

Taking a single gap barbell resonant cavity as an example. Figure 6 shows the frequency of the first three modes varied with *w*. It can be seen that the frequency of the fundamental mode TM_{110} is scarcely influenced by *w*, which is consistent with the operating principle of the barbell cavity. However, things are different for the high order modes. The frequency of TM_{210} and TM_{310} decreases with *w* increased. Therefore, although good uniformity of the electric field can be obtained in terms of the operating principle of the barbell cavity, the increase of the transverse size will significantly reduce the frequency interval between the fundamental mode and the adjacent high order modes. Thus, the mode competition becomes fiercer.

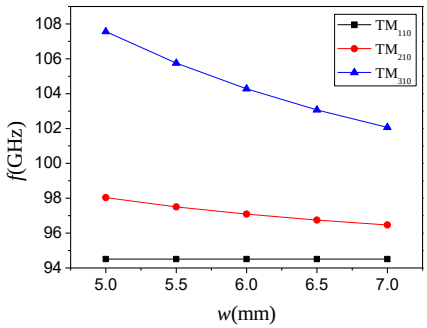

Figure. 6 Frequency of the first three modes in a single gap barbell cavity varied with w.

The high order mode devices are promising because the size of devices decreases sharply with the frequency increased. Taking TM_{210} as an example, which is an antisymmetric mode, the distribution of the field is strongest near the coupling cavities and zero at the center. Figure 7 shows the field when two beam tunnels are introduced at the region of the strongest electric field.

ISSN 2616-5767 Vol.4, Issue 3: 58-63, DOI: 10.25236/AJETS.2021.040307

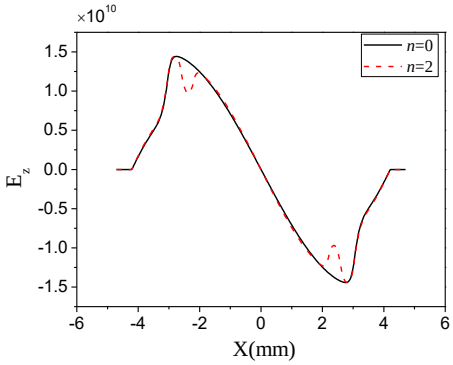

Figure. 7 Transverse field distribution of TM210 in a planar two-beam barbell resonant cavity.

3.2. Axial mode

In order to improve the characteristic impedance of the cavity, multigap cavity should be adopted where the axial modes will exist. For a *n*-gap cavity, there are *n* axial modes with the same transverse mode which can be denoted as 0(2π), π/(*N*-1), 2π/(*N*-1), …, π. The different axial modes will overlap each other, which results in a very complex mode competition.

Figure 8 shows the mode spectrum of a three-gap cavity. It can be seen that the number of modes increases from 3 to 6 in the cavity with the frequency ranged from 94.5GHz to 104.32GHz. Therefore, the frequency interval between adjacent modes is reduced and the mode competition of the cavity is more prominent.

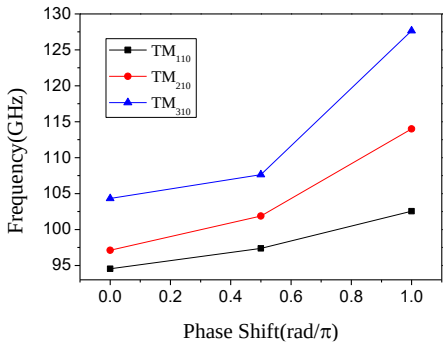

Figure. 8 Mode spectrum of a three-gap barbell cavity.

4. Analysis of coupling coefficient of the cavity

Coupling coefficient is an important concept which represents the synchronization characteristics of the standing wave field and the electron beam. It can be defined as

$$M = \frac{\left|\int_{-\infty}^{\infty} E_c(z) e^{j\beta_e z} dz\right|}{\int_{-\infty}^{\infty} \left|E_c(z)\right| dz} \tag{1}$$

where E_c (*z*) is the distribution function of the electric field.

Figure 9 shows the normalized field of axial electric field for TM_{110} along different tunnels in a three-gap cavity. It can be seen that for TM_{110}-2π and TM_{110}-π/2, the electric field distribution of different beam tunnels is exactly the same but only differing from the amplitude. For the TM_{110}-π mode, except for the different amplitude, the electric field in different tunnels are opposite in phase. However, the electric field in the tunnels 3 and 3' will be exactly the same as that of the other tunnels 1, 2 and 2' when it is negative.

ISSN 2616-5767 Vol.4, Issue 3: 58-63, DOI: 10.25236/AJETS.2021.040307

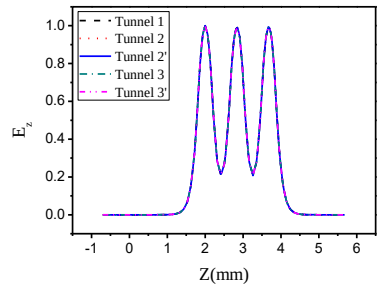

(a) TM_{110}-2π

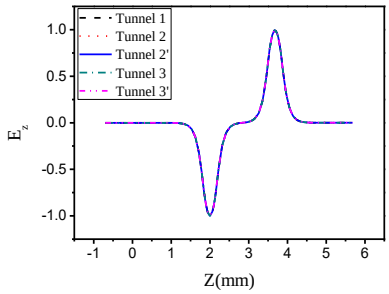

(b) TM_{110}-π/2

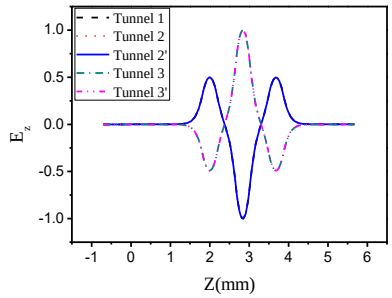

(c) TM_{110}-π

Figure. 9 Normalized field distribution of E_z along the center of each electron beam tunnel.

From Figure 9, it can be seen that the fields of different electron beam tunnels can be described by the same field shape function which are only different in their complex coefficients. Thus, the axial electric field of the *i*-th tunnel can be written as follows

$$E_{c,i}(z) = \dot{V}_{m,i} F(z) \tag{2}$$

where the field shape factor $F(z)$ satisfies the normalization condition

$$L\int_0^L F^2(z)dz = 1 \tag{3}$$

Therefore,

$$L\int_0^L E_{c,i}^2(z)dz = \dot{V}_{m,i}\dot{V}_{m,i}^* \tag{4}$$

Gap voltage is defined as:

$$V_i = \int_0^L \left|E_{c,i}(z)\right| dz = \left|\dot{V}_{m,i}\right| \int_0^L \left|F(z)\right| dz \tag{5}$$

Therefore, interaction electric field of any one mode can be represented by a normalized field factor $F(z)$ and a set of complex coefficients $\left(\dot{V}_{m,1}, \dot{V}_{m,2}, \cdots, \dot{V}_{m,N}\right)$. And the field shape factor $F(z)$ can be constructed by the field in any tunnel.

Taking formula (2) into (1), we can obtain

ISSN 2616-5767 Vol.4, Issue 3: 58-63, DOI: 10.25236/AJETS.2021.040307

$$M = \frac{\left|\int_{-\infty}^{\infty} F(z) e^{j\beta_e z} dz\right|}{\int_{-\infty}^{\infty} \left|F(z)\right| dz} \tag{6}$$

By analyzing formula (6), it can be seen that the coupling coefficient can be entirely determined by the field distribution function $F(z)$ when the voltage is determined. That is, the coupling coefficient is independent of tunnel distribution because the field shape factor $F(z)$ is the same for all tunnels. The conclusion is obvious in physics, because the coupling coefficient represents the synchronization characteristic in the multigap cavity which is determined by the operating voltage and circuit period. Both of them are independent of the tunnel distribution.

5. Conclusions

The high frequency characteristics of planar multi-beam barbell cavity are studied in the paper, including the introduction of beam tunnel, mode distribution and field shape. We have found that the number of beam tunnels is limited by the uniformity of the electric field and the work stability. Thus, the tunnel spacing should be considered seriously in the design. Mode distribution is the most difficult problem in the design of the cavity. The stability of the cavity can not be guaranteed only by the design of operating mode due to the existence of multiple modes in both transverse and longitudinal directions. Finally, in order to describe the electric field distribution of the different tunnels, the normalized field shape factor and complex coefficient are introduced. For a certain mode, the field distribution of different tunnels actually satisfies the same distribution function only with different complex coefficient. This is of great significance to study the stability of planar multi-beam barbell cavity theoretically.

Acknowledgements

This work was supported in part by Beijing Natural Science Foundation under Grant 1192007, in part by the Scientific Research Project of Beijing Educational Committee under Grant KM202010017010, and in part by the Institute of Nano-Photoelectronics and High Energy Physics.

References

[1] M. Chodorow, T. Wessel-Berg(1961), A high-efficiency klystron with distributed interaction[J], IRE Trans. Electron Devices, 8(1): 44-55.
[2] B. Levush, D.K. Abe, J.P. Calame, B.G. Danly, K.T. Nguyen, E.J. Dutkowski, R.H. Abrams, R.K. Parker(2007), Vacuum Electronics: Status and Trends[J], IEEE A&E Systems Magazine, 22(9): 28-34.
[3] A. Srivastava (2018), Design of a 10kW W-band Sheet Beam Extended Interaction Klystron[J], European Journal of Advances in Engineering and Technology, 5(11): 852-857.
[4] J. Pasour, E. Wright, K.T. Nguyen, F.N. Wood, R.E. Myers, B. Levush(2014), Demonstration of a multikilowatt, solenoidally focused sheet beam amplifier at 94 GHz[J], IEEE Transactions on Electron Devices, 61(6): 1630–1636.
[5] S. Chen, C. Ruan, Y. Wang, C. Zhang, D. Zhao, X. Yang, S. Wang(2014), Particle-in-cell simulation and optimization of multigap extended output cavity for a W-band sheet-beam EIK[J], IEEE Transactions on Plasma Science, 42(1): 91–98.
[6] S. Lü, C. Zhang, S. Wang, Y. Wang (2015), Stability Analysis of a Planar Multiple-beam Circuit for W-band High Power Extended-interaction Klystron[J], IEEE Transactions on Electron Devices, 62(9): 3042-3048.
[7] R. Dobbs, A. Roitman, P. Horoyski, M. Hyttinen, D. Sweeney, D. Chernin, M. Blank, N.S. Barker, J. Booske, E. Wright, J. Calame, O.V. Makarova(2010), Fabrication Techniques for a THz EIK[C], IEEE IVEC, 2010: 181-182.
[8] D. Gamzina, L.G. Himes, R. Barchfeld, Y. Zheng, B.K. Popovic, C. Paoloni, E. Choi, N.C. Luhmann(2016), Nano-CNC Machining of Sub-THz Vacuum Electron Devices[J], IEEE Transactions on Electron Devices, 63(10): 4067-4073.